DEPARTMENT OF THE INTERIOR

U.S. GEOLOGICAL SURVEY

FLUID-ROCK INTERACTION AND FRACTURE DEVELOPMENT IN 'CRYSTALLINE' ROCK TYPES

by

D. E. Moore, C. A. Morrow, and J. Byerlee[1]

Open-File Report 87-279

[1] U.S. Geological Survey, 345 Middlefield Road
Menlo Park, California 94025

INTRODUCTION

This report represents both a data base for and an expansion of our permeability and fluid-rock interaction studies on 'crystalline' rocks at elevated temperatures. Moore _et al._ (1983) studied the changes in permeability and fluid chemistry as water was flowed down a temperature gradient through samples of Westerly and Barre granite. Morrow _et al._ (1985) conducted similar permeability experiments at 250°C maximum temperature on samples of anorthosite, gabbro, and quartzite, and they compared the results with the equivalent earlier experiment for Westerly granite. This paper presents a more thorough discussion of the fluid chemistry results than was contained in Morrow _et al._ (1985), and it expands the comparison to include two 250°C permeability experiments on Barre granite. The entire set of fluid chemistry results are contained here; only selected results were included in previous papers.

A petrographic description is also provided for each of the rock types used in the 'crystalline' rock permeability experiments. The major focus of the petrographic work was to identify the various natural alteration assemblages and to determine their distribution in each rock, to aid in the interpretation of the fluid chemistry results. Brief descriptions of fracture development in all five rock types are also included, for application to the permeability data. In order to better relate the fluid chemistry to the rock chemistry, compositions of the major minerals in the gabbro and anorthosite were also obtained using electron microprobe techniques.

Mineralogy and Textures of Rock Types

The starting materials of the five rock types studied show many variations in texture, primary and alteration mineral assemblages, and mineral composition. Table 1 summarizes the mineralogy of these rocks. Tables 2-5 present average compositions of the major minerals in the anorthosite, gabbro, and Westerly and Barre granites, respectively. The quartzite sample consists almost exclusively of quartz and the few alteration minerals of variable composition are extremely fine-grained; therefore, mineral analyses have not been obtained for that rock type. Data for the gabbro and anorthosite were collected using an ARL SEMQ 9-channel, fully automated electron microprobe at the U.S.G.S. in Menlo Park, California. The mineral data for the two granodiorites were obtained earlier using an ARL EMX-SM, 3-channel electron microprobe at Stanford University (Moore et al., 1983). The relative proportions of ferrous and ferric iron in a given mineral cannot be determined using electron microprobe techniques. Therefore, total iron in an analysis is reported as FeO or Fe_2O_3, in accordance with the valence state that usually predominates in the mineral.

A brief mineralogical and textural description of each rock type is given below, with emphasis on the distribution of alteration minerals and the development of fractures.

Anorthosite

The anorthosite samples come from a large anorthosite inclusion within a diabase body at Split Rock, near Duluth, Minnesota. The inclusion consists almost completely of plagioclase crystals that are largely fresh and unaltered, tabular in shape, and relatively coarse-grained. Individual

Table 1.

Comparative Mineralogy of Crystalline Rock Types

(Symbols: 1-Primary igneous or sedimentary mineral; 2-alteration or vein mineral; X-abundant mineral, occupying more than 10 volume percent of rock; Tr-trace mineral; ?-before number, identity of mineral uncertain and after number, time of crystallization uncertain; Ser.-sericite)

Mineral	Gabbro	Anorthosite	Westerly Granite	Barre Granite	Quartzite
Quartz				1X	1X1X
Plagioclase (An≥10)	1X	1X	1X	1X	
K-feldspar			1X	1X	?1Tr
Muscovite			1 2(Ser.)	1 2(Ser.)	2Tr
Biotite 1	2*		1	1	2?Tr
Clinopyroxene	1				
Orthopyroxene	1	1Tr			
Olivine		1			
Magnetite	1 2Tr	1Tr	1Tr 2Tr	1Tr	2Tr
Apatite	1Tr		1Tr	1Tr	2Tr
Zircon			1Tr	1Tr	1Tr
Tourmaline			1Tr	1Tr	
Fluorite			2Tr		
Sphene			1Tr 2Tr	1Tr 2Tr	
Calcite			2	2Tr	2Tr
Chlorite	2	2Tr	2Tr	2Tr	
Albite (An<5)				2	
Epidote			2Tr	2	
Pumpellyite		?2Tr			
Lawsonite					?2Tr
Mesolite		2			
Iddingsite	2				
Amphibole	2				
Talc	2				

*also phlogopite

Table 2. Average compositions of minerals in the anorthosite.

	(An_{77}) Plagioclase	(Fs_{38}) Hypersthene	(Fs_{25}) Bronzite	Vein Mineral Mesolite?
SiO_2	49.5	52.2	53.7	40.7
TiO_2		0.4	0.3	----
Al_2O_3	32.5	1.2	1.6	29.2
Fe_2O_3				----
FeO		23.4	16.6	
MgO		21.6	26.5	----
MnO		0.4	0.3	----
CaO	15.5	0.9	0.6	11.6
Na_2O	2.5	----	----	3.5
K_2O	0.1			
Anhydrous Total	100.1	100.1	99.6	85.0
Si	2.26	1.95	1.95	8.20
Al^{IV}	1.74	0.05	0.05	6.93
Al^{VI}		0.02	0.02	
Ti		0.01	0.01	----
Fe^{3+}				----
Fe^{2+}		0.73		0.50
Mg		1.20	1.44	----
Mn		0.01	0.01	----
Ca	0.76	0.03	0.02	2.50
Na	0.22	----	----	1.38
K	0.004			
Oxygens (anhydrous)	8	6	6	30

Abbreviations: An-anorthite; Fs-ferrosilite (numbers after abbreviations indicate percentage of the end-number compositions indicated).

Table 3. Average compositions of minerals in the gabbro.

	(An_{66}) Plagioclase	Augite	(Fs_{34}) Hypersthene	(Fa_{43}) Olivine	Iddingsite	Chlorite	Pale-Green Amphibole	Dark Green Amphibole	Talc	Biotite	Phlogopite
SiO_2	51.8	53.0	52.7	34.9	44.2	29.8	50.4	43.4	59.9	37.8	40.2
TiO_2	0.1	0.1	0.3	----	0.1	----	0.2	0.1	----	5.6	1.9
Al_2O_3	30.4	0.6	0.7	----	0.5	15.0	4.1	10.6	0.3	12.7	13.1
Fe_2O_3	0.5				35.0						
FeO		8.6	21.5	36.8		21.1	16.7	23.6	6.6	14.2	7.7
MgO	0.1	14.3	22.7	27.5	9.4	19.5	13.7	6.8	26.4	14.7	21.5
MnO	----	0.2	0.5	0.5		0.2		0.4			
CaO	13.4	22.7	1.3	0.1	0.9	0.2	11.0	11.4	0.1	----	----
Na_2O	3.7	0.1	0.1	0.1	0.1	0.1	1.1	1.9	0.1	0.1	0.3
K_2O					----		0.1		----	9.9	10.1
Anhydrous Total	100.0	99.6	99.8	99.9	90.2	85.9	97.3	98.2	93.4	95.0	94.8
Si	2.35	1.98	1.97	0.98		6.26	7.45	6.66	7.96	5.67	5.83
Al^{IV}	1.63	0.02	0.03	----		1.74	0.55	1.34	0.04	2.25	2.17
Al^{VI}						1.98	0.15	0.57	0.01		0.07
Ti	----	0.01	0.01	----		----	0.02	0.01	----	0.63	0.20
Fe^{3+}	0.02										
Fe^{2+}		0.27	0.67	0.87		3.71	2.07	3.03	0.73	1.77	0.94
Mg	0.01	0.80	1.26	1.16		6.10	3.02	1.55	5.23	3.29	4.65
Mn	----	0.01	0.01	0.01		0.03		0.05			
Ca	0.65	0.91	0.05	----		0.04	1.74	1.88	0.02	----	0.01
Na	0.33	0.01	----	----		0.04	0.32	0.57	0.03	0.03	0.08
K							0.01		----	1.90	1.87
Oxygens (anhydrous)	8	6	6	4		28	23	23	22	22	22

Abbreviations: An-anorthite; Fs-ferrosilite; Fa fayalite

Table 4. Average compositions of minerals in Westerly Granite.

	Plagioclase Cores (An_{17})	Plagioclase Rims (An_9)	K-feldspar	Muscovite	Biotite	Chlorite	Epidote
SiO_2	63.7	64.6	65.4	48.5	37.2	26.2	37.5
TiO_2	----	----	0.1	0.1	2.6	0.1	0.2
Al_2O_3	22.8	22.2	18.5	28.6	15.9	19.1	23.5
Fe_2O_3	0.1	0.1	0.1	5.8			14.0
FeO					19.8	27.6	
MgO	----	----	----	1.8	9.8	13.9	----
MnO						0.5	0.3
CaO	3.7	1.9	----	----	0.1	0.1	22.8
Na_2O	9.2	10.3	0.8	0.2	0.1		----
K_2O	0.3	0.3	15.1	10.6	8.2	0.1	
Anhydrous Total	99.8	99.4	100.0	95.6	93.7	87.6	98.3
Si	2.82	2.86	3.01	6.51	5.73	5.63	2.98
Al^{IV}	1.19	1.16	1.00	1.49	2.27	2.37	0.02
Al^{VI}				3.03	0.61	2.45	2.18
Ti	----	----	----	0.01	0.30	0.01	0.01
Fe^{3+}	----	----	----	0.59			0.84
Fe^{2+}					2.54	4.95	
Mg	----	----	----	0.36	2.26	4.43	----
Mn						0.08	0.02
Ca	0.17	0.09	—	—	0.01	0.02	1.94
Na	0.79	0.89	0.07	0.05	0.02		----
K	0.02	0.01	0.89	1.82	1.60	0.02	
Oxygens (anhydrous)	8	8	8	22	22	28	12.5

Abbreviations: An-anorthite

Table 5. Average compositions of minerals in Barre Granite.

	Plagioclase Cores (An_{13})	Plagioclase Rims (An_3)	(An_1) Albite	K-feldspar	Muscovite	Biotite	Chlorite	Epidote
SiO_2	65.1	67.7	68.5	64.9	47.3	36.7	26.3	37.7
TiO_2	----	----	----	----	0.6	2.7	0.1	0.4
Al_2O_3	21.8	20.0	19.6	18.5	30.5	16.2	19.7	24.7
Fe_2O_3	0.1	----	0.2	——	4.0			12.2
FeO						20.9	29.0	
MgO	----	----	----	----	1.8	8.7	12.4	0.1
MnO							0.6	0.1
CaO	2.8	0.7	0.4	----	——	----	0.1	23.0
Na_2O	9.8	11.2	11.3	0.6	0.3	0.1		----
K_2O	0.3	0.2	0.1	15.8	10.8	9.8	0.1	
Anhydrous Total	99.9	99.8	100.1	99.8	95.3	95.1	88.3	98.2
Si	2.87	2.97	2.99	2.98	6.35	5.66	5.63	2.98
Al^{IV}	1.13	1.03	1.00	1.03	1.65	2.34	2.37	0.02
Al^{VI}					3.18	0.60	2.60	2.28
Ti	----	----	----	----	0.06	0.31	0.01	0.02
Fe^{3+}	----	----	0.01	----	0.41			0.72
Fe^{2+}						2.69	5.19	
Mg	----	----	----	----	0.37	1.99	3.95	0.01
Mn							0.10	0.01
Ca	0.13	0.03	0.02	——	——	——	0.01	1.95
Na	0.85	0.95	0.96	0.06	0.06	0.01		——
K	0.02	0.02	0.01	0.93	1.84	1.93	0.03	
Oxygens (Anhydrous)	8	8	8	8	22	22	28	12.5

Abbreviation: An-anorthite

crystals range from about 0.5 to 10 cm in length; they are bytownites of average composition An_{77} (Table 2). Small, fresh orthopyroxene crystals of bronzite composition (Table 2) are found along some of the plagioclase grain boundaries, and a few rounded orthopyroxene crystals containing fine-grained opaques occur as inclusions within some of the plagioclase crystals. The orthopyroxene inclusions are hypersthenes with slightly higher Fe/Mg ratios than the interstitial pyroxenes.

Most of the alteration in the anorthosite is concentrated along numerous fractures. The major set of filled fractures forms a sub-parallel array, and a subsidiary set is oriented at about 60-75° to the first one. Figure 1a shows the major group of fractures, one of which is relatively wide and filled with a mineral whose habit varies from fibrous to tabular. In several places, short fractures filled with alteration minerals extend out from the main fractures into adjoining plagioclase crystals (Fig. 1b). According to Grout and Schwartz (1939), the principal vein mineral is kaolinite; however, the fibrous vein mineral in our samples is a Ca-Na zeolite with composition close to mesolite (Table 2). Scattered, rounded aggregates of a very fine-grained, greenish-colored, high-relief mineral are minor components of the veins (Fig. 1b); this mineral may be pumpellyite. Some of the orthopyroxene inclusions in plagioclase are partly altered to mesolite and/or chlorite.

The plagioclase crystals in the anorthosite also contain many minor, intragranular cracks; in contrast to the major fracture sets, the orientation of these small cracks commonly shows a crystallographic control. The majority of these cracks originate at the grain boundaries and extend for various distances into the plagioclase crystals; examples of these cracks are shown in Figures 2 and 3. Unlike the major fractures, which are commonly filled with the zeolite mineral, many of the minor cracks appear to be empty.

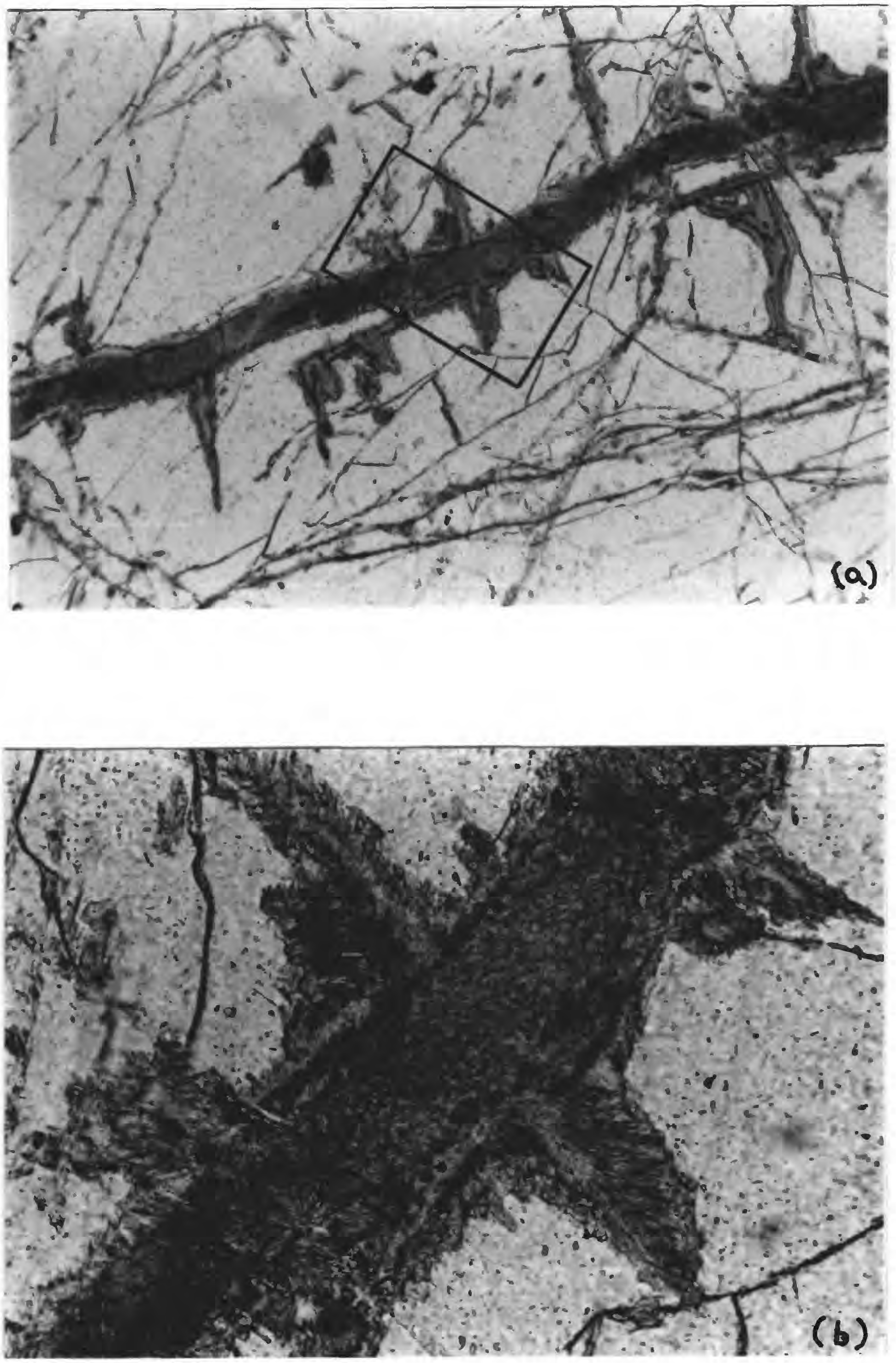

Figure 1. (a). Mineral-filled fractures in anorthosite (Scale: 3.5 mm horizontal dimension). (b). Close-up of boxed area in (a), showing fibrous mesolite-filled vein and nearly perpendicular offshoots of veins into surrounding plagioclase crystals (Scale: 0.9 mm horiz. dim.; both photos in plane polarized light).

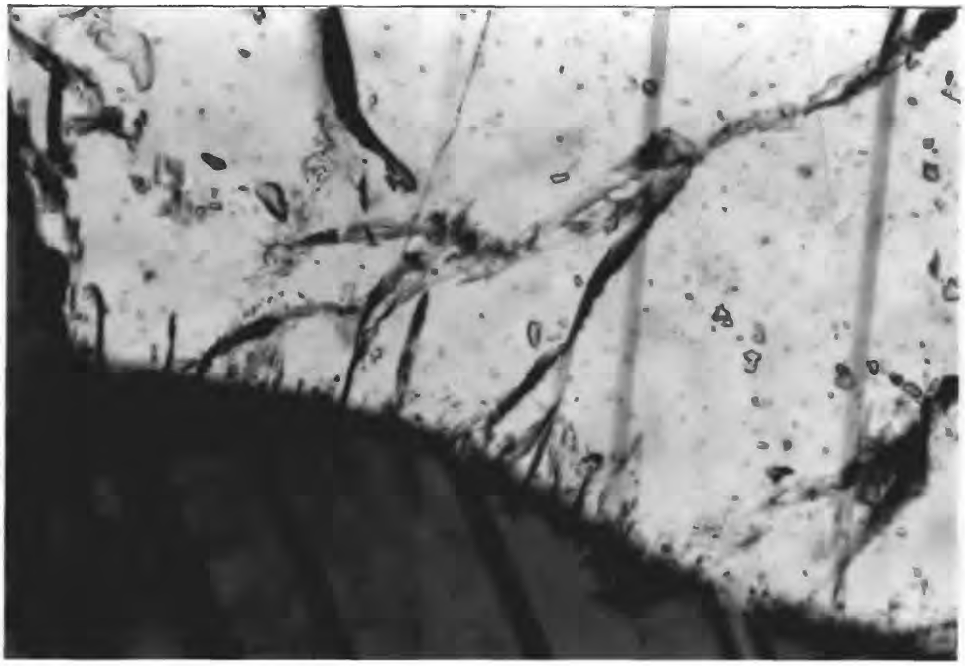

Figure 2. Small fractures in anorthosite that extend into plagioclase crystals from grain boundaries. Many of the fractures are oriented approximately perpendicular to the grain boundary (Scale: 0.56 mm horiz. dim.; crossed polarizers).

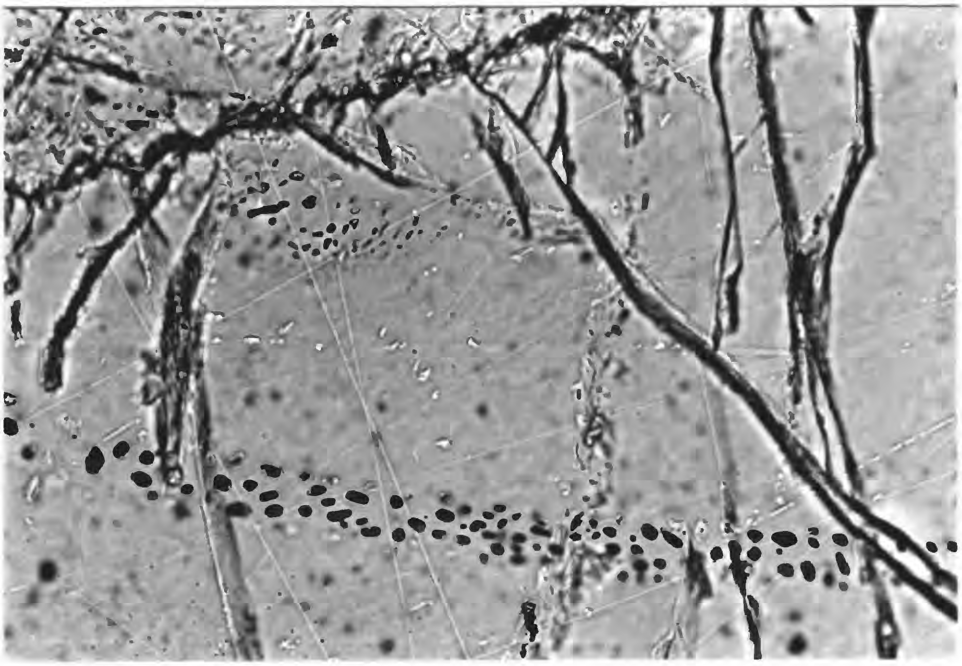

Figure 3. Small fractures along plagioclase grain boundaries in anorthosite. A plane of fluid inclusions crosses the lower part of the photo (Scale: 0.35 mm horiz. dim.; plane polarized light).

The grain boundaries seen in Figures 2 and 3 are relatively well defined; a different type of grain boundary is shown in Figure 4. In this case there is no sharp break between adjacent crystals but rather a zone of gradual transition. These boundary zones characteristically contain a series of tabular inclusions that may be large fluid inclusions. The arrow in Figure 4 points to two inclusions that appear to be in the process of pinching off to form smaller ones. These zones may represent original grain boundary cracks that have healed through the precipitation of plagioclase.

Gabbro

The gabbro samples come from the mafic intrusive complexes of Minnesota. Gabbroic rocks of the Duluth Gabbro Complex can be divided into two groups that were intruded at different times (Taylor, 1964). The samples used in this study most closely resemble the spotted gabbro that forms part of the younger and volumetrically more important group of intrusives. Tabular plagioclase crystals up to 15 mm in length comprise 50 to 60 volume percent of the sample. Much of the plagioclase is twinned and compositionally zoned; the average composition is that of a labradorite with anorthite content of An_{66} (Table 3). Some of the plagioclase crystals are partially enclosed in poikilitic crystals of augitic clinopyroxene (Table 3) and magnetite. The gabbro also contains some orthopyroxene crystals of hypersthene composition and many rounded olivine crystals with average composition $Fa_{43}Fo_{57}$ (Table 3). The orthopyroxene apparently formed by inversion from pigeonite, and it shows exsolution lamellae (Taylor, 1964).

The plagioclase is only slightly altered; however, some of the pyroxene and much of the olivine shows complex replacement by secondary minerals (Tables 1 and 3). A cluster of partly altered mafic grains is shown in

Figure 4. Healed plagioclase-plagioclase grain boundary in anorthosite. Elongate fluid inclusions are oriented perpendicular to the original grain boundary. Arrow points to two inclusions that are in the process of pinching off to form smaller inclusions (Scale: 0.28 mm horiz. dim.; plane polarized light).

Figure 5. Olivine shows various degrees of replacement by iddingsite ± phlogopite ± opaques, ranging from minor alteration along the outer edge and fractures to total replacement. Pyroxenes are replaced by combinations of pale to dark blue-green amphibole and chlorite. Some completely altered grains show a core of talc, a concentric zone of pale amphibole, and an outer rim of chlorite. There is a complete range of compositions between colorless phlogopite and deep red biotite (Table 3), and the entire compositional range can be found in individual crystals. These micas are commonly associated with the amphibole alteration. The boundary between altered mafic grains and plagioclase is characteristically marked by a zone of chlorite and the chlorite commonly extends partway into the plagioclase along short fractures (Fig. 5). Figure 6 shows a closer view of some chlorite-filled fractures whose orientations are controlled by the cleavage and twinning directions of the plagioclase.

As seen in Figures 5 and 6, most of the fractures in the gabbro are short segments that are completely contained within a single crystal. Most of these minor fractures are filled with alteration minerals such as chlorite, and they show a crystallographic control in that they follow cleavage and twinning directions of the containing feldspar crystals (Fig. 6). There is a modestly developed, sub-parallel set of fractures in these samples; individual fractures in this set rarely cross more than 4 or 5 grains, however. One somewhat wider (up to 0.1 mm) and more extensive, chlorite-filled fracture is oriented approximately perpendicular to the main fracture set.

Quartzite

This sample was collected from the Death Valley area, California. In contrast to the two mafic rocks that lack quartz as either a primary or

Figure 5. Cluster of olivine and pyroxene crystals in gabbro that are partly altered to combinations of phlogopite, talc, iddingsite, calcic amphibole, and chlorite. Chlorite-filled fractures extend a short distance into surrounding plagioclase crystals (Scale: 2.2 mm horiz. dim.; crossed polarizers).

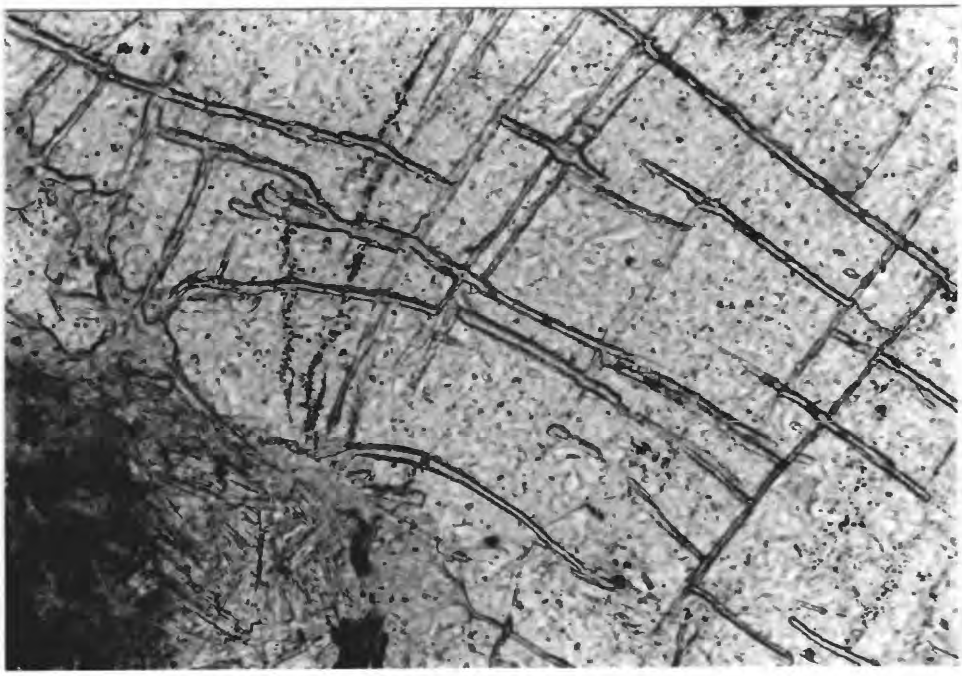

Figure 6. Chlorite-filled fractures extending from altered mafic mineral into plagioclase crystals of gabbro. Fracture orientations follow cleavage and twinning directions of the feldspar (Scale: 0.9 mm horiz. dim.; plane polarized light).

secondary mineral, the quartzite consists almost exclusively of equigranular quartz that averages 0.3 mm in diameter. The quartz crystals characteristically show wavy extinction and sutured grain boundaries (Fig. 7). Several of the smaller quartz grains are partly polygonized. The quartzite contains only trace amounts of other minerals; the most important ones are magnetite that occurs as small idioblastic crystals scattered throughout the rock, and white mica that replaces a few clasts (originally K-feldspar?) and that also occurs as a vein-filling mineral. There are also scattered occurrences of apatite and calcite, and a few high-relief crystals that may be lawsonite.

The quartzite starting material contains only a few, mineral-filled fractures. One of these is shown in Figure 7. Those portions of the fractures that cut through quartz crystals are relatively straight, whereas the portions that follow the sutured grain boundaries are very irregular. These main fractures tend to be segmented, with adjoining segments overlapping slightly. In a few places the fractures are anastomosing. The fractures are filled with white mica, calcite, and opaque minerals; calcite appears to have been the last mineral to crystallize. The quartzite also shows an array of sub-parallel fluid inclusion trails. Some relatively short trails can be seen in Figure 7; the longer ones may extend across 4 or 5 quartz grains. These fluid inclusion trails may represent healed fractures.

Westerly and Barre Granite

The Westerly and Barre granites of Rhode Island and Vermont, respectively, have been extensively quarried, and both rock types are commonly used in experimental studies. Although they are informally called granites, both rocks classify as granodiorites based on their mineral proportions. The two granodiorites have very similar primary and secondary mineral assemblages, but

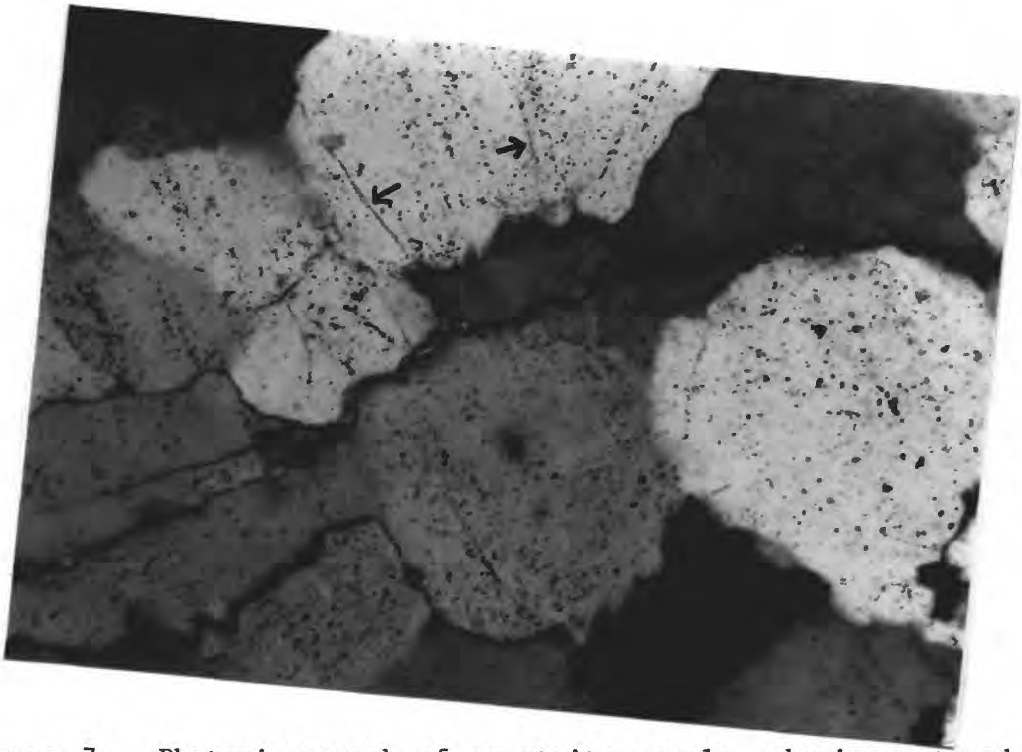

Figure 7. Photomicrograph of quartzite sample, showing sutured grain boundaries and a fracture that is filled with muscovite and calcite. The fracture is very irregular where it follows grain boundaries. Arrows point to short fluid inclusion trails within single quartz crystals (Scale: 0.9 mm horiz. dim.; crossed polarizers).

their textures are somewhat dissimilar. The primary igneous minerals in both rock types consist of plagioclase, quartz, K-feldspar, biotite, and muscovite with accessory magnetite, apatite, zircon, sphene, and tourmaline. The plagioclase in both rocks is compositionally zoned, with oligoclase cores and albite rims; both the core and rim compositions of the Westerly plagioclase are slightly enriched in calcium compared to the Barre plagioclase (Tables 4 and 5). The biotite in Westerly has a greenish-brown color and it is slightly enriched in magnesium and depleted in iron and potassium compared to the reddish-brown biotite in Barre. The primary muscovite in Westerly has slightly lower aluminum and higher iron contents than that of Barre (Tables 4 and 5).

Minor amounts of calcite, chlorite, epidote, and sphene occur as alteration minerals in both rocks; Westerly also contains fluorite and Barre contains fine-grained albite as secondary minerals. Plagioclase in both rock types is partly replaced by sericitic muscovite, calcite, and, more rarely, epidote, chlorite, and sphene. The plagioclase in Westerly generally contains a greater abundance of alteration minerals than that of Barre. The alteration in plagioclase tends to be concentrated in specific compositional zones or along cleavage and twin planes. Biotite in both rocks is partly altered to chlorite + sphene + epidote; in Westerly, minor amounts of fluorite and magnetite are associated with the altered biotite, whereas in Barre some plagioclase adjacent to such biotite is replaced by aggregates of fine-grained albite. The relative iron and magnesium contents of the chlorite in the two granodiorites reflect the biotite compositions in those rocks. Similar to the muscovite, the epidote in Westerly has slightly lower aluminum and higher iron contents than that in Barre (Tables 4 and 5).

Overall, Westerly is a medium-grained rock; it consists of subhedral plagioclase crystals up to 2.2 mm long that are commonly mantled by K-feldspar, and somewhat smaller (about 1 mm diameter) anhedral quartz and anhedral to subhedral K-feldspar. Mafic minerals and their alteration products are evenly distributed throughout the rock. The Westerly samples examined are not foliated, and the quartz and feldspar crystals are not highly strained; grain boundaries tend to be smooth and regular. Barre is much coarser-grained than Westerly; and it is dominated by large (up to 3.5 mm long), anhedral, and highly strained quartz and K-feldspar crystals that wrap around smaller (0.8-1 mm diameter) grains of quartz, plagioclase, and mafic minerals. Many of the quartz-quartz grain boundaries in Barre are sutured, and several of the quartz-feldspar and feldspar-feldspar boundaries are also irregular. Some of the large quartz and feldspar grains have broken down to finer-grained aggregates of the same minerals.

The samples of Westerly and Barre used in this study do not contain any major fractures, but several minor ones can be found, particularly in quartz. Some examples of fractures in quartz are shown for Barre in Figure 8 and for Westerly in Figure 9. The two fractures in Figure 8 are not simple breaks but rather consist of clusters of small fractures, some of which intersect at low angles whereas others are arranged in a slightly overlapping en echelon pattern. Some fractures are filled with fine-grained muscovite (Fig. 9); muscovite also occurs along quartz-quartz and quartz-feldspar grain boundaries. Calcite also commonly is deposited in fractures and along grain boundaries in these samples.

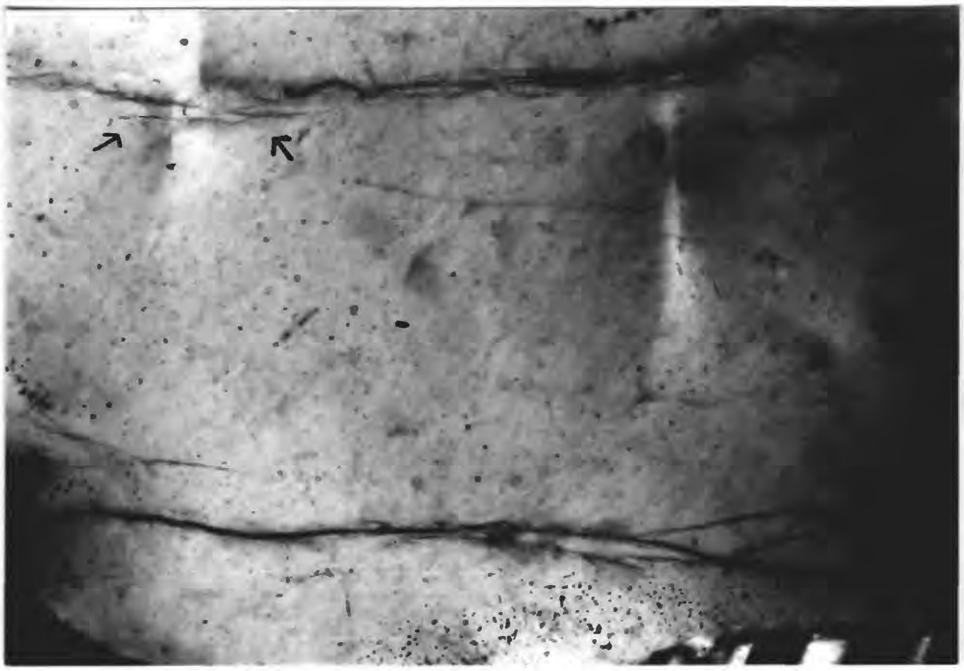

Figure 8. Fracture networks developed in a quartz crystal in Barre. Each major fracture is composed of many short segments, some of which intersect at low angles and others of which are in an en echelon pattern (indicated by arrows) (Scale: 0.9 mm horiz. dim.; crossed polarizers).

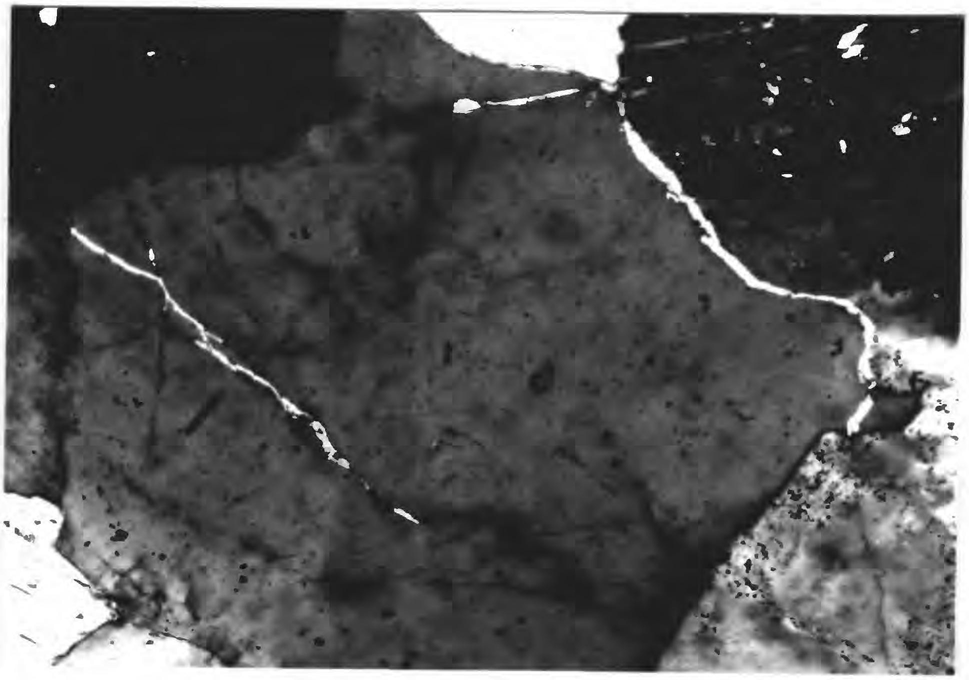

Figure 9. Intragranular and grain-boundary fractures in Westerly; bright portions of the fractures shown are filled with muscovite (Scale: 0.9 mm horiz. dim.; crossed polarizers).

PERMEABILITY

A permeability experiment was conducted at 250°C borehole temperature, 30 megapascals (MPa) confining pressure, 10 MPa pore pressure, and 0.5 MPa differential pressure for each of the five rock types. The experimental apparatus and procedures are described in Moore et al. (1983); the apparatus is shown in Figure 10. Permeability was measured as fluids were forced from the higher-temperature borehole to the lower-temperature outer edge of a rock cylinder that was 7.6 cm in diameter and 8.9 cm long. The changes in permeability with time after the samples were heated are shown in Figure 11; in Figure 12 the permeability changes for a given sample are normalized relative to the initial heated permeability of that sample to allow direct comparison of the different experiments.

The following features of the permeability results were noted in previous studies:

--- All of the samples showed decreases in permeability with time.

-- Comparison of the Westerly and Barre results suggested that the amount of permeability decrease was directly correlated with the volume of fluid that flowed through the samples (Moore et al., 1983).

--- Morrow et al. (1985) emphasized the importance of quartz in relation to the size of the permeability reduction.

--- The permeability decreases in the crystalline rocks were considered by Morrow et al. (1985) to be caused by their low porosities and pore sizes.

Addition of the data from the two 250°C permeability experiments on Barre granite to the data from the other samples studied by Morrow et al. (1985) leads to some additional conclusions:

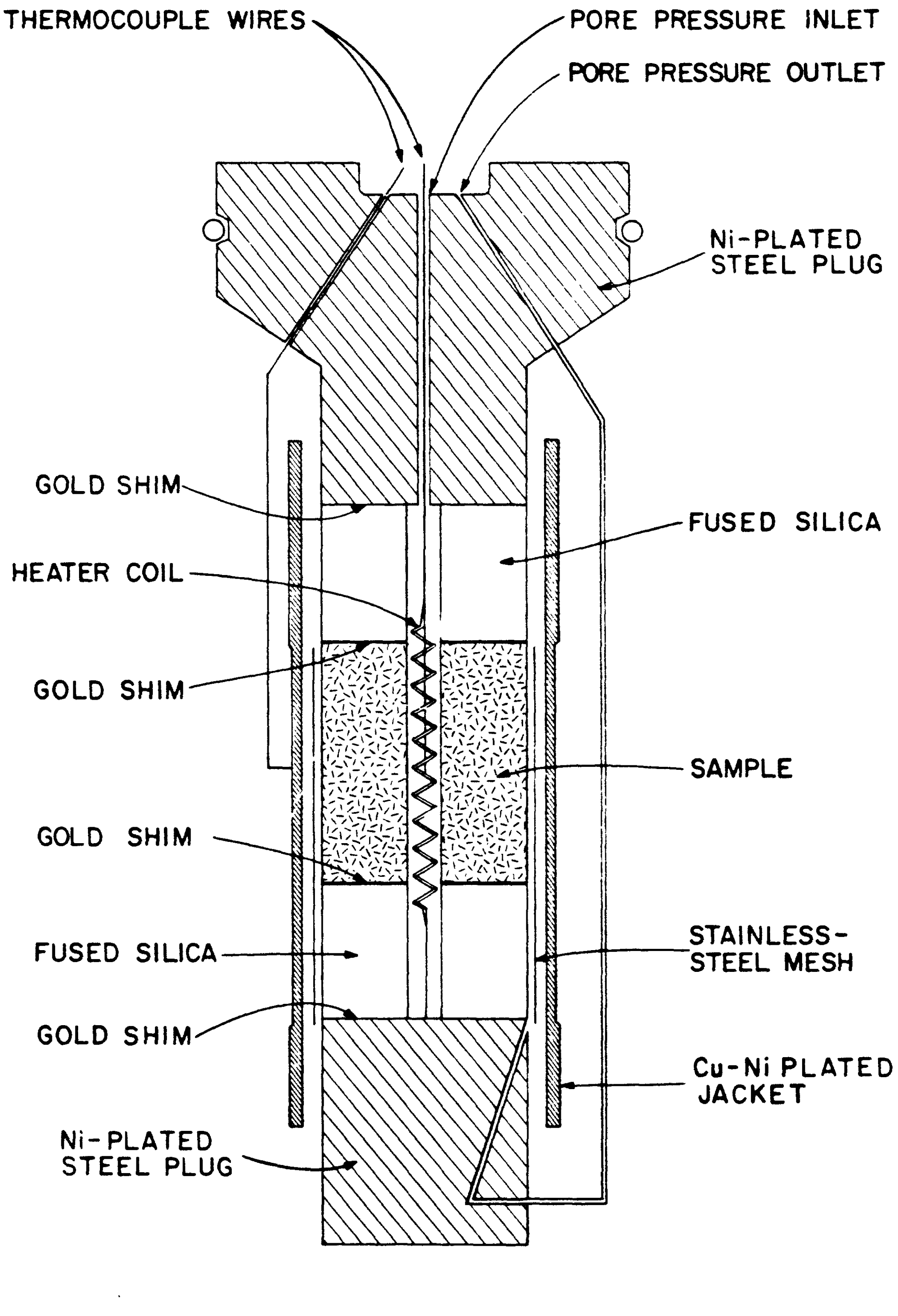

Figure 10. Experimental apparatus.

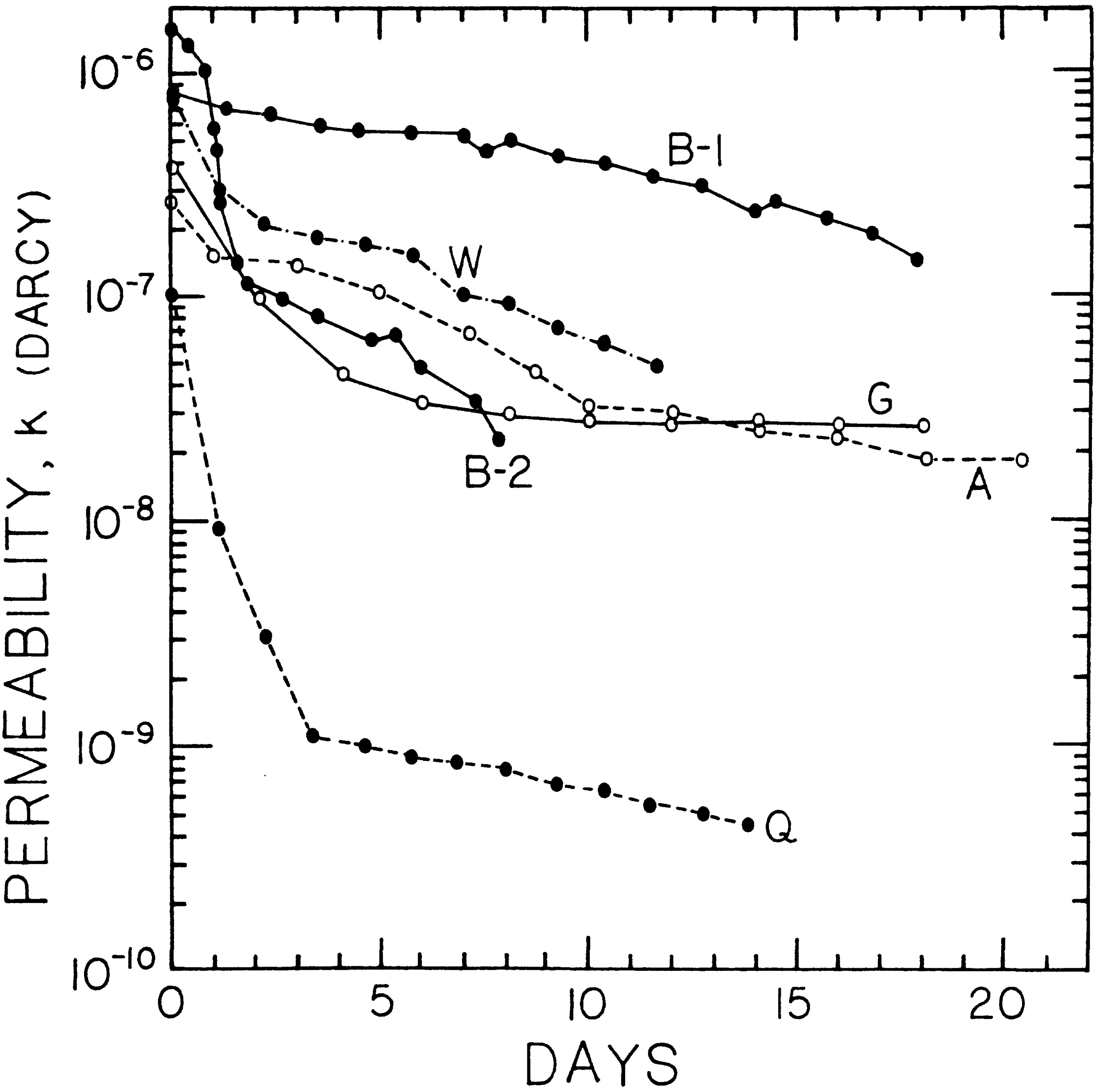

Figure 11. Changes with time in the permeability of the heated rock samples. (1 darcy = 0.987 x $10^{-12}m^2$)

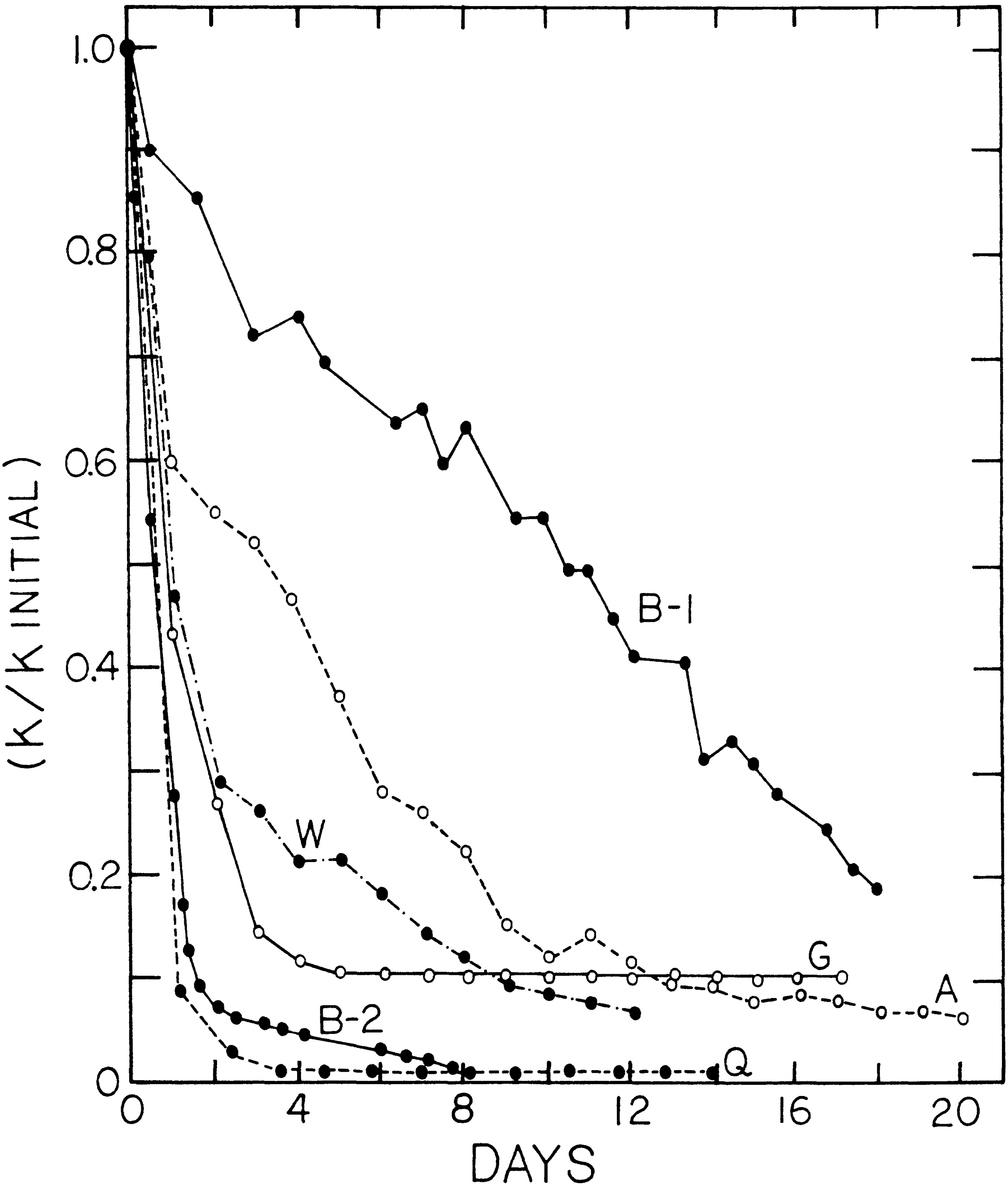

Figure 12. Changes in permeability normalized with respect to the initial permeability of each sample.

1) The initial heated permeability values of the samples (Fig. 11) show a correlation with the rock type. The three granodiorite samples have higher initial permeabilities than the gabbro and anorthosite, and the quartzite sample has the lowest initial permeability. Because of the small number of samples, it is difficult to know whether this indicates a general trend in permeability relative to rock type. Certainly, the sample-to-sample variation for a given rock type is also large, as demonstrated by the two samples of Barre (Fig. 11).

2) To some extent, the different initial permeability values can also be correlated with their textural properties. The very low quartzite permeability is certainly a result of the sutured grain boundaries and the scarcity of fractures. The fractures that are present are relatively tortuous in places (Fig. 7), and they are also filled with mineral deposits. Many preexisting fractures in the quartzite also were closed by crack-healing processes, as indicated by the planes of fluid inclusions. Many grain-boundary cracks in the anorthosite have been healed, and most of the fractures in the gabbro are filled with alteration minerals. In contrast, both Barre and Westerly contain numerous unfilled fractures, particularly in quartz; and fluid flow in Westerly was considered by Vaughan _et al._ (1986) to be concentrated in quartz-rich areas.

3) The first Barre (B-1) sample provides an apparent exception to the conclusion of Morrow _et al._ (1985) that the amount of permeability decrease is correlated with the quartz content of the rock. The behavior of this sample is consistent, however, with the earlier conclusion of Moore _et al._ (1983) that the amount of permeability decrease is correlated to the fluid volume.

The relatively constant rate of permeability change during the B-1 experiment is also quite different from the other experiments. Because the permeability of the B-1 sample was continuing to decrease at the end of the experiment, the proportional permeability change for this sample would have been as high as for the other quartz-bearing samples if it had been continued for a longer time.

FLUID CHEMISTRY

During the permeability experiments, the fluids discharged from the low-temperature outer edge of the samples were collected at intervals for chemical analysis. The complete fluid chemistry results obtained for the six experiments are listed in Table 6. Selected results have been presented in Moore _et al._ (1983) and Morrow _et al._ (1985); sample collection and analytical techniques are outlined in Moore _et al._ (1986). Deionized water was the starting fluid in all cases. Although the borehole temperature was the same in each experiment, the jacket temperature varied from sample to sample, due in part to differences in the thermal conductivity of the rocks tested. The jacket temperature for each experiment is listed in Table 6.

The following features of the fluid chemistry results were noted in the two previous reports:

--- All of the rock samples contained a finite amount of ionic material that was readily leached from the samples by room-temperature deionized water (see Table 6). This material may represent some combination of groundwaters, fluid inclusions, and ions or salts that are loosely adhered to mineral surfaces (Moore _et al_., 1983). For most of the experiments, an initial room-temperature flushing

Table

Compositions of fluids collected during equivalent experiments on 5 crystalline rock types. Experimental Conditions: Confining pressure-30 MPa; pore pressure-10 MPa; differential pore pressure-0.5 MPa; borehole temperature-250°C. Concentrations are in mg/L. (Note: The Barre, Westerly, and quartzite experiments were run before the techniques were developed for aluminum analyses; therefore, aluminum is not discussed in the text.)

Experiment	Days	Cumulative flow (ml)	pH	SiO_2	Na	K	Mg	Ca	Al	HCO_3	SO_4	HPO_4	Total F	Cl
Anorthosite														
Room-T	0		6.5	7	31	20	1.2	6.6	0.15	79	7.0	---	0.84	31
	3.9		6.7	12	9.2	12	0.46	4.0	0.04	42	1.3	---	0.62	8.1
	-0-	-0-												
Heated	1.0	11.6	6.8	35	13	7.3	0.60	11	0.43	61	2.1	---	0.54	8.2
(Jacket Temp = 61°C)	2.0	20.0	6.7	63	13	5.3	0.64	7.8	0.04	54	1.8	0.09	0.45	7.1
	3.0	30.0	6.4	73	13	4.3	0.48	5.0	0.08	46	1.7	0.99	0.35	4.5
	4.0	39.9	6.7	74	12	3.7	0.39	4.3	0.11	40	1.8	0.64	0.18	2.8
	6.9	57.7	6.7	66	12	3.7	0.37	2.3	0.10	39	2.3	0.85	0.18	2.4
	8.9	67.8	6.6	66	12	3.2	0.36	4.3	0.50	35	1.9	1.1	0.16	1.7
	10.9	73.1	6.6	62	11	3.2	0.35	2.9	0.03	35	1.8	2.3	0.14	2.2
	15.9	82.8	6.5	68	12	3.4	0.40	2.2	0.09	36	1.8	----	0.14	1.5
	20.9	91.0	6.6	69	12	3.8	0.42	3.2	0.05	46	0.8	----	0.21	2.2

Table 6 (continued)

Experiment	Days	Cumulative flow (ml)	pH	SiO_2	Na	K	Mg	Ca	Al	HCO_3	SO_4	HPO_4	Total F	Cl
<u>Gabbro</u>														
<u>Room-T</u>	1.8		6.5	17	11	7.1	0.99	5.7	0.02	57	2.3	1.7	0.34	7.3
	5.6		6.5	20	13	2.8	0.73	5.0	0.07	57	2.3	2.7	0.70	6.0
	-0-	-0-												
<u>Heated</u>	2.0	16.9	7.0	50	43	2.4	0.27	1.5	0.73	74	3.3	1.4	0.55	5.1
(Jacket temp. 62°C)	3.0	20.5	7.1	46	33	2.2	0.31	1.9	0.16	76	2.7	1.7	0.32	4.6
	4.3	23.6	6.9	48	34	2.0	0.40	1.2	0.05	76	2.5	1.4	0.40	4.5
	6.1	27.6	7.1	55	36	2.0	0.35	0.76	0.06	76	2.5	5.4	0.32	4.8
	8.0	33.5	7.1	70	33	1.7	0.27	0.76	0.07	69	2.0	3.7	0.31	3.7
	17.0	50.4	7.2	80	33	1.1	0.24	0.38	0.18	67	1.2	3.2	0.40	3.2
<u>Westerly Granite</u>														
<u>Room-T</u>	0		6.2		16	20	17	2.0						
	0.89		5.0											
	1.91		6.5		49	61	22	1.5		120	25	----	3.4	63
	2.66		6.8	4	51	82	20	1.2			---	----	2.2	46
	3.66		5.8	3.4	3.8	12	2	0.6		1.5	---	----	1.3	22
	-0-	-0-												

Table 6 (continued)

Experiment	Days	Cumulative flow (ml)	pH	SiO_2	Na	K	Mg	Ca	Al	HCO_3	SO_4	HPO_4	Total F	Cl
<u>Heated</u>	1.0	31.0	6.8		34	13	3.9	53			18	----	3.5	82
(Jacket temp. 84°C)	1.1	35.8	7.3	210						110	18	----	3.1	83
	1.3	38.4	7.8		35	12	4.0	52			18	----	3.3	76
	1.9	48.8	7.1	210						120	17	----	3.4	61
	2.1	51.5	6.9		35	12	3.6	49			15	----	3.6	62
	2.2	54.3	7.0	210						140	13	----	3.3	61
	2.9	64.4	7.2	200	34	12	3.0	44						
	3.1	67.0	7.0	230						120	12	----	2.9	48
	3.3	69.3	6.7		32	11	2.9	38			12	----	3.0	49
	4.0	77.3	6.8	230						110	10	----	2.7	43
	4.1	78.3	7.7		30	9.6	2.5	36			8	----	2.8	40
	5.1	89.2	7.6	250	27	9.0	2.1	33			9	----	2.5	36
	6.0	100.0	7.3	230						110	8	----	3.0	29
	6.2	103.1	7.7		28	8.0	2.6	32			10	----	3.1	30
	6.9	108.6	6.9	230						110	7	----	3.2	28
	7.3	110.6	7.6		27	8.0	1.9	33			6.4	----	3.0	26

Table 6 (continued)

Experiment	Days	Cumulative flow (ml)	pH	SiO_2	Na	K	Mg	Ca	Al	HCO_3	SO_4	HPO_4	Total F	Cl
	7.9	115.1	7.4	210						110	7	----	2.8	23
	8.9	120.5	7.2	180	28	7.6	1.9	31			7	----	3.1	21
	10.0	125.0	7.2	180						130	8	----	3.5	21
	11.0	129.8	7.6		32	9.7	2.1	33		130	7	----	3.8	22
	11.9	134.2	7.7	180						140	7	----	3.7	19
<u>Barre-Granite-1</u>														
	-0-	-0-												
<u>Heated</u>	2.1	3.4	7	94	190	46	5.3	220		140	80	----	10	720
(Jacket temp.= 80°C)	3.2	4.5	7		170	37	2.7	160		140	53	----	11	490
	4.0	7.5	7		150	29	1.6	110		130	38	----	11	360
	5.0	11.3	7		140	20	1.0	88		120	32	----	11	280
	6.0	14.9	7	140	120	17	1.3	64		120	29	----	14	250
	7.0	18.6	7		110	14	0.56	46		120	19	----	11	170
	8.0	21.6	7	150	100	12	0.33	38		110	20	----	14	150
	9.2	24.8	7		92	10	0.32	28		110	16	----	12	120
	10.1	27.8	7	150	85	10	0.21	24		100	13	----	13	100

Table 6 (continued)

Experiment	Days	Cumulative flow (ml)	pH	SiO_2	Na	K	Mg	Ca	Al	HCO_3	SO_4	HPO_4	Total F	Cl
	11.0	30.0	7		81	9.4	0.60	26		97	12	----	12	86
	12.0	32.4	7	150	75	8.2	0.25	19		96	12	----	12	83
	13.0	34.4	7		75	8.4	0.16	19		94	9.8	----	11	73
	14.1	36.4	7	160	70	6.6	0.08	18		96	9.3	----	13	73
	15.2	38.2	7		67	6.6	0.10	19		99	9.0	----	12	66
	18.0	41.8	7	160	64	6.8	0.37	18		97	11	----	11	61
<u>Barre Granite-2</u>														
<u>Room-T</u>	0		6.6	16	42	25	1.9	26		87	94	----	2.2	49
	0.8		7.0	20	91	40	2.3	58		190	220	----	2.7	74
	1.1		7.3	24	64	31	1.7	38		130	120	----	2.0	53
	1.8		7.7	20	59	22	0.7	26		84	100	----	2.2	24
	2.0		7.4	20	52	22	0.7	24		78	83	----	1.9	23
	2.8		7.3	20	34	18	0.5	21		61	51	----	1.5	19
	-0-	-0-												
<u>Heated</u>	0.2	14.4	7.4	220	35	23	1.1	27		94	49	----	1.6	25
(Jacket temp. = 103°C)	0.9	62.0	7.6	320	26	16	0.6	23		84	21	----	1.4	17

Table 6 (continued)

Experiment	Days	Cumulative flow (ml)	pH	SiO_2	Na	K	Mg	Ca	Al	HCO_3	SO_4	HPO_4	Total F	Cl
	2.2	81.3	7.7	220	35	20	0.6	25		110	23	----	2.5	17
	3.0	86.9	7.7	200	42	19	0.6	26		130	23	----	3.1	15
	4.1	92.5	7.9	190	46	16	0.4	21		150	22	----	3.9	13
	4.9	96.2	7.7	180	48	12	0.2	22		160	22	----	4.6	14
	6.0	100.6	7.5	180	51	18	0.3	23		170	20	----	5.1	17
	7.0	103.4	7.5	130	51	15	0.5	21		160	18	----	5.2	18
Quartzite														
Room-T	0.08		6.9	5.9	24	16	1.6	12						
	0.14		6.3	4.5										
	0.19		6.2	2.5										
	8.0		6.8	21	4.1	3.7	0.63	9		24	11	----	0.22	1.8
	12.0		6.8	21	4.5	4.0	0.51	9		22	10	----	0.34	1.8
	-0-	-0-												
Heated	2.0	12.8	7.0	240	14	12	1.7	29		69	30	----	0.45	9.0
(Jacket temp. = 111°C)	14.9	15.2	6.8	170	16	12	2.4	37		94	45	----	0.85	12

procedure was conducted to remove the majority of this material prior to heating. This was done so that the compositions of the heated fluids would principally reflect mineral dissolution and/or precipitation reactions. The flushing procedure was not done for the Barre-1 experiment; as a result, the first few fluid samples contain a large component of the readily removed salts (Moore *et al.*, 1983; see Table 6).

--- The compositions of the heated fluids discharged from Barre and Westerly granites were in part functions of flow rate and temperature, (Moore *et al.*, 1983).

--- Comparison of the heated fluid compositions from Barre and Westerly granites showed that: (1) the higher Mg contents of the Westerly fluids were consistent with the higher Mg contents of biotite and chlorite in that rock; and (2) the higher Na concentrations and Na/Ca ratios of the Barre fluids corresponded to the higher albite component of the plagioclase in Barre (Moore *et al.*, 1983).

--- Dissolved silica concentrations in the Westerly and Barre experiments showed trends with time that were different from those of many of the other species. The concentrations of most of the dissolved species were considered to reflect dissolution reactions alone, whereas silica may have been involved in precipitation as well as dissolution reactions. As flow rates decreased concomitant with the permeability reductions, the silica-precipitation reactions became more important (Moore *et al.*, 1983).

--- The heated fluids collected from the anorthosite and gabbro were more dilute than those collected from the quartzite, and, particularly, from Westerly.

--- All the fluids were nearly neutral, with those from the anorthosite having the lowest pH and those from Westerly having the highest pH (Morrow et al., 1985).

Before making additional comparisons, certain features of the quartzite experiment should be noted. The quartzite and other rock cylinders were wrapped in a stainless steel screen before being placed in the jacket. The presence of the screen allowed fluids to exit the sample and move to the outlet lines. Approximately 10 milliliters (ml) water could collect in the volume provided by the mesh of the screen. Fluids newly discharged from the rock cylinder would mix with the other water in the screen, and the compositions would reflect this mixing. Because of its extremely low permeability, considerably less water flowed through the quartzite sample than through the other rock types. Only about 2.5 ml water was discharged from the quartzite cylinder in the 13 days that elapsed between collection of the first and second fluid samples. Therefore, the final fluid composition reported for the quartzite sample (Table 6; Figures 13-18) reflects the presence of a large component of earlier discharged fluids, so that measured compositional changes between the first and second samples are not as pronounced as the actual changes in the final discharged fluids.

Comparison of the combined fluid and mineral data for all five rock types yields some additional conclusions about the chemical reactions taking place, as described below.

Silica. Figure 13 shows the changes with time in dissolved silica concentrations. A clear correlation can be seen between mineralogy and dissolved silica content, in that the fluids from the three quartz-bearing rock types have significantly higher silica concentrations than those from the gabbro and anorthosite, both of which rock types lack quartz. Because the

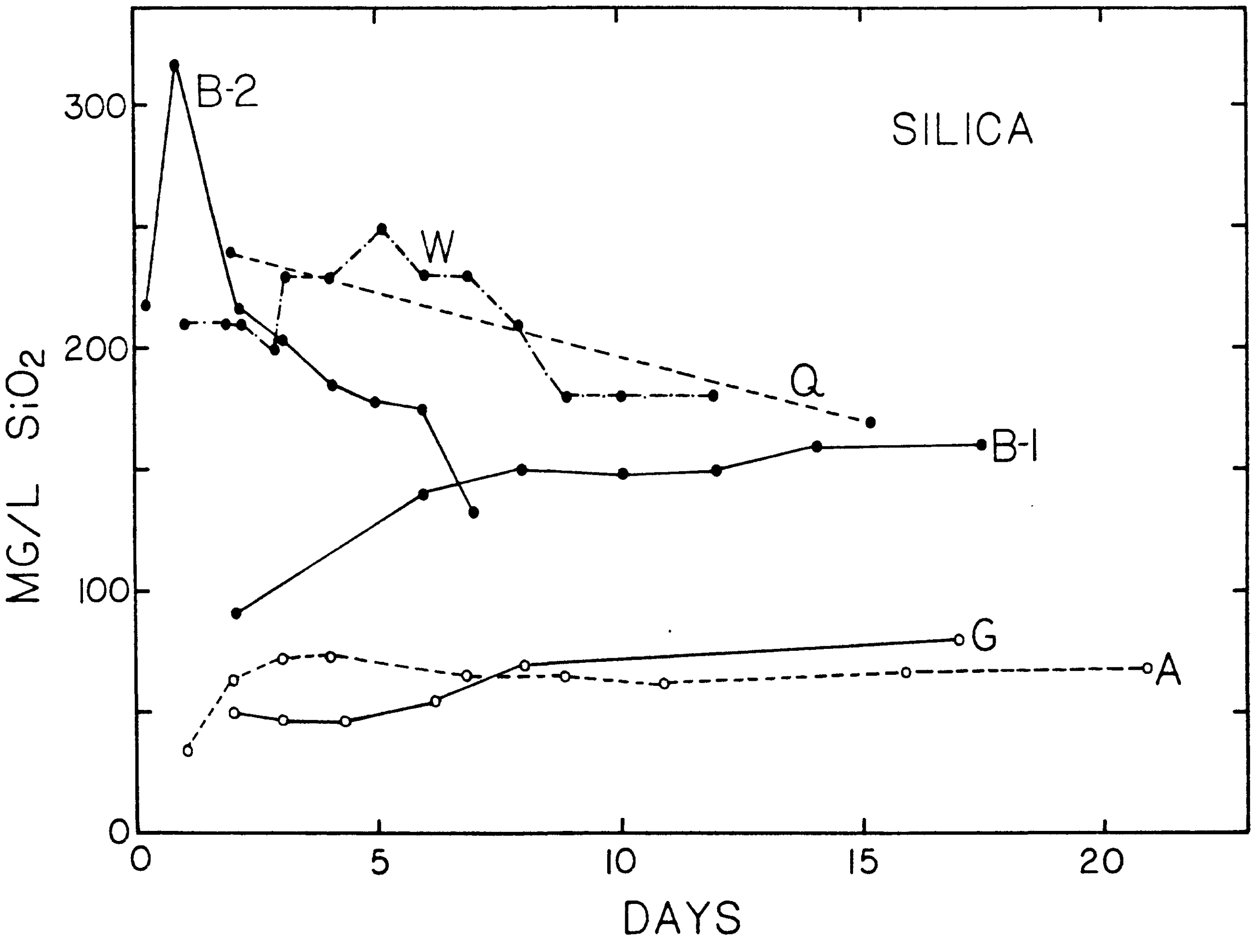

Figure 13. Changes with time in the dissolved silica contents of the fluids discharged during the permeability experiments.

amount of silica in solution was found to be a function of flow-rate, the silica contents of fluids from the quartz-bearing samples might have decreased significantly if the experiments had been conducted for longer periods of time.

Bicarbonate. As with silica, bicarbonate concentrations in the discharged fluids (Fig. 14) are higher for the granodiorites and the quartzite, all of which contain calcite as a vein and alteration mineral. Some of the granodiorite experimental products show etched calcite in the borehole area (Moore et al., 1983), which indicates that calcite was being dissolved during the experiments. The Westerly and Barre-2 fluids show increases in bicarbonate contents near the ends of the experiments, and the final bicarbonate concentrations of all three granodiorite experiments are inversely related to their permeability.

Calcium. Calcium concentrations in solution (Fig. 15) show no relationship to the anorthite content of plagioclase in the four plagioclase-bearing rocks (Tables 2-5). This is in contrast to the previous conclusion of Moore et al. (1983). For example, the gabbro and anorthosite have plagioclase compositions averaging An_{66} and An_{77}, respectively, yet the final heated calcium concentrations for both rocks are below 5 mg/L. In contrast, Barre and Westerly contain plagioclase with oligoclase cores (An_{10-20}) and albite rims and the quartzite contains no observable traces of calcic plagioclase; nevertheless, these three rock types produced relatively large amounts of dissolved calcium (e.g., 20-30 mg/L Ca final concentrations). The elevated calcium concentrations in Westerly, Barre, and the quartzite are, correlated with the presence of calcite in those rocks (Table 1). In the Westerly and Barre-2 experiments, however, the calcium concentrations decrease with time whereas the bicarbonate contents show an overall increase. These different

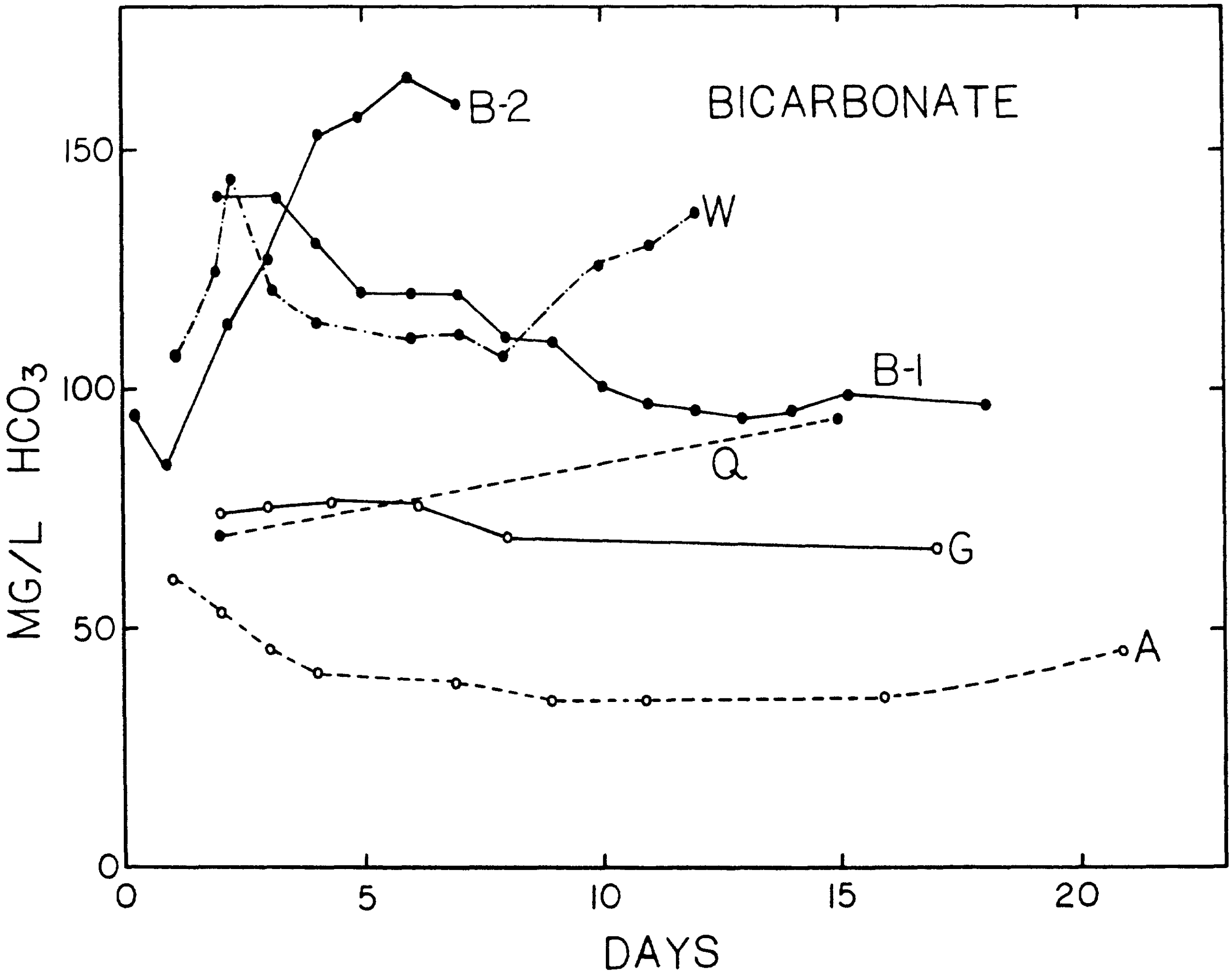

Figure 14. Bicarbonate contents of the fluids discharged during the crystalline rock permeability experiments.

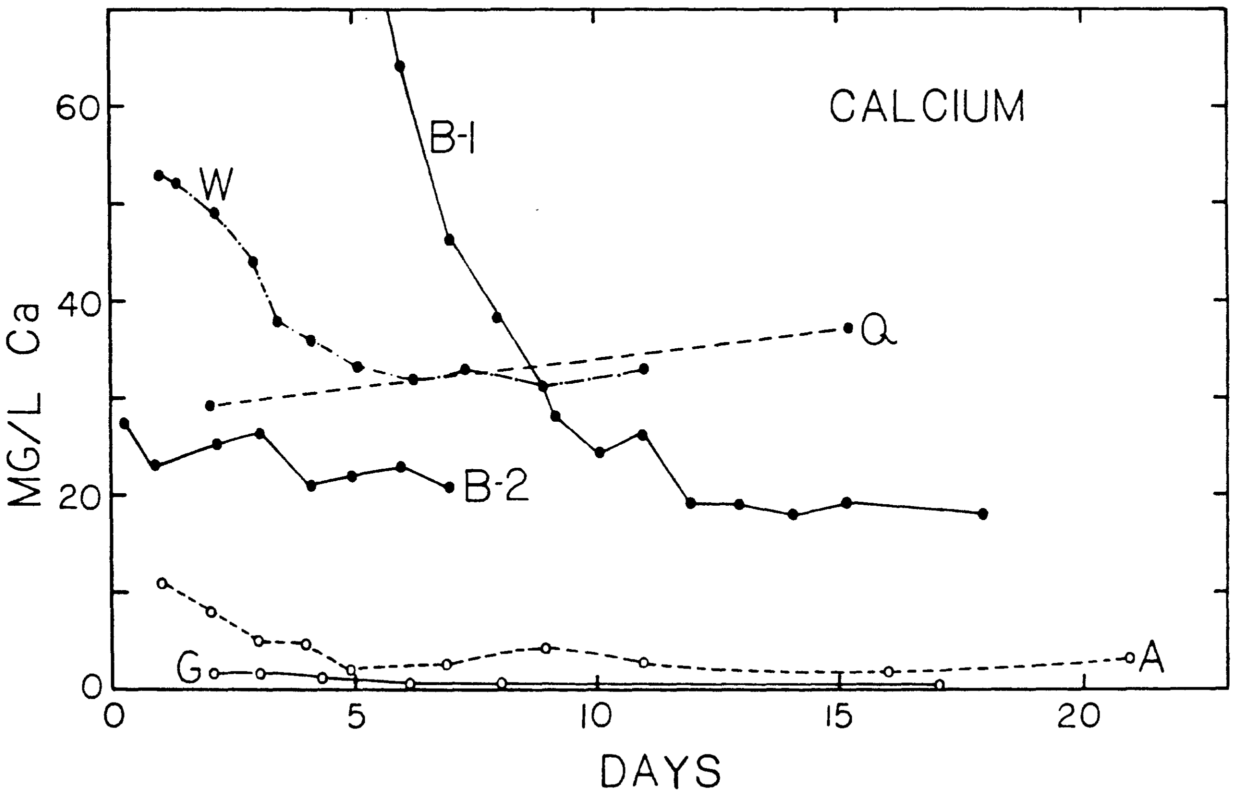

Figure 15. Calcium contents of the discharged fluids.

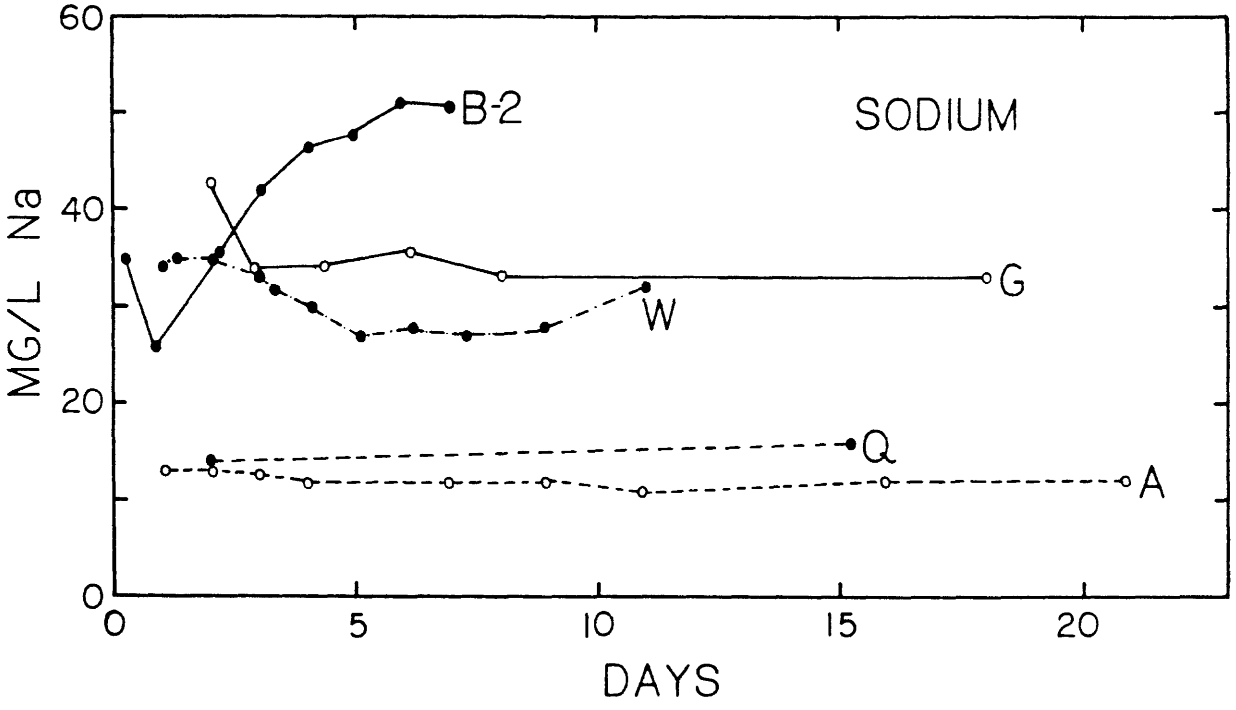

Figure 16. Changes with time in the sodium contents of the fluids discharged during the permeability experiments.

different trends may indicate that some of the calcium that was released to the fluids from calcite dissolution was reprecipitated in some other mineral, perhaps a calcium zeolite. Morrow et al. (1981) observed calcium-bearing fibers, possibly of a zeolite mineral, that were deposited on plagioclase crystals during an experiment on Westerly.

Sodium. The quartzite and anorthosite fluids have considerably lower sodium concentrations than the Barre, Westerly, and gabbro fluids (Fig. 16). The principal mineral source of sodium in solution is the albite component of plagioclase, which is found in all of the rocks except the quartzite. This would explain the relatively low sodium concentrations in the quartzite fluids. The sodium that is present in those fluids is probably derived from residual pore fluids left after the room-temperature flushing procedure. The low sodium contents of the anorthosite fluids are not readily explained, because the anorthosite consists almost exclusively of sodium-bearing plagioclase. A possible explanation is that the low dissolved sodium concentrations result from the incorporation of this ion into the sodium-bearing zeolite mesolite.

Potassium. Potassium concentrations in the discharged fluids (Fig. 17) are directly correlated with the presence of K-feldspar and muscovite in the rocks. Biotite and phlogopite are apparently not very soluble in low-temperature hydrothermal fluids, hence the low potassium contents of the gabbro fluids. Although potassium concentrations of the gabbro and anorthosite fluids are very low, potassium actually occurs in higher concentrations than calcium in those two experiments. In the granodiorite and quartzite samples, calcium concentrations are higher than potassium in all the heated fluid samples.

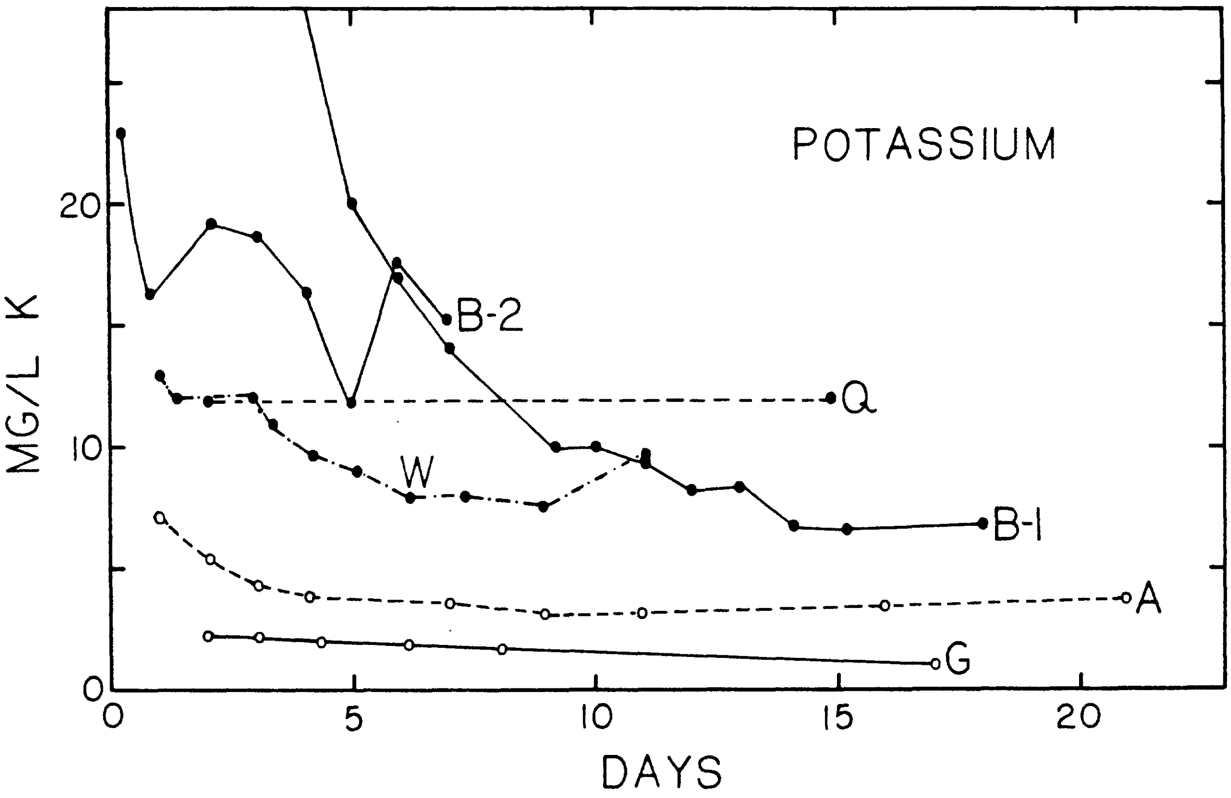

Figure 17. Potassium contents of the discharged fluids.

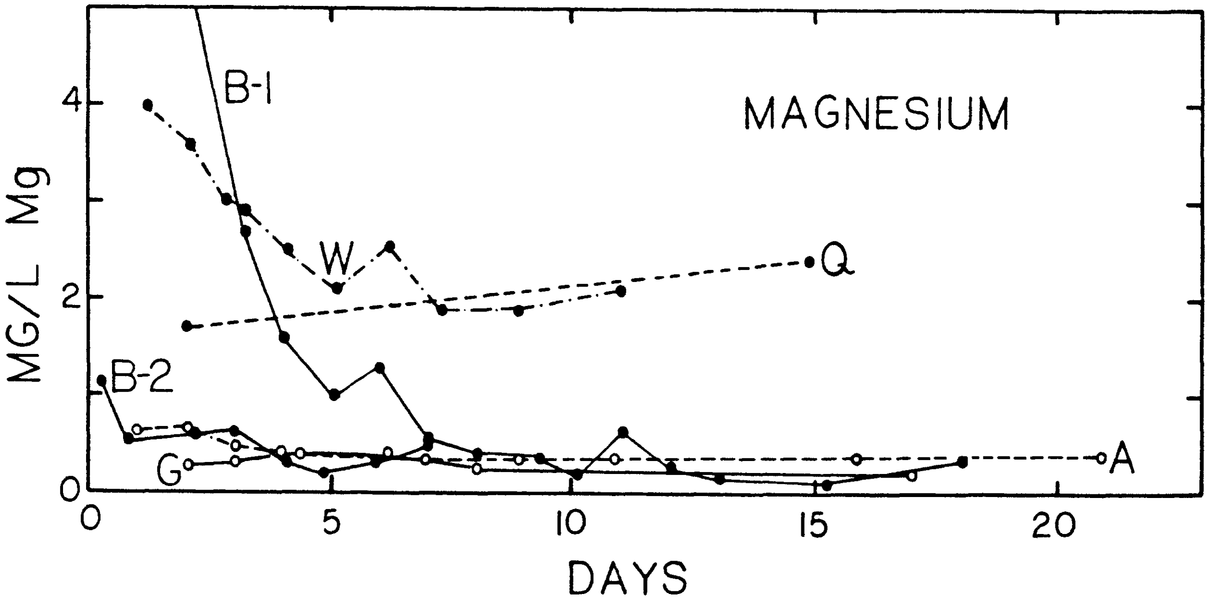

Figure 18. Changes with time in the dissolved magnesium concentrations of the discarged fluids.

Magnesium. The variations in magnesium concentration with time for the experiments are shown in Figure 18. The amount of magnesium in solution appears to have very little correlation with the mineralogy and mineral compositions of the rock samples. This is in contrast to the previously described correspondence between solution magnesium concentrations and the magnesium contents of biotite and chlorite in Westerly and Barre (Moore et al., 1983). The gabbro contains biotite and chlorite with much higher magnesium contents than those of Westerly and Barre, yet the gabbro fluids have very low magnesium concentrations. It is likely that the relatively high Westerly and quartzite dissolved magnesium concentrations are due to the incorporation of some magnesium in the calcite, which is much more soluble than most ferromagnesian minerals.

Other Anions. The changes in the amounts of fluoride, chloride, sulfate, and phosphate ion in solution during the experiments are listed in Table 6. Sulfate and chloride are the most highly concentrated of these four anions overall, and their initial concentrations in Barre and Westerly fluids are relatively high. With time, however, the concentrations decrease markedly to low values. Sulfate remains high in the quartzite, but with greater amounts of fluid flow it would probably also have decreased. Sulfate and chloride are also relatively abundant in the room-temperature fluids collected, and Moore et al. (1983, 1986) considered that these two anions were principally derived from interstitial pore fluids and possibly fluid inclusions. The decreases in these two anions with time during the permeability experiments would reflect depletion of the sources of these ions.

Phosphate ion was not found in the Westerly, Barre, or quartzite fluids, but it forms a small component of the anorthosite fluids and a more important part of the gabbro fluids. In contrast, fluoride ion concentrations are low in the gabbro, anorthosite, and quartzite fluids but relatively high in the Barre and Westerly fluids. Unlike sulfate and chloride, the concentrations of phosphate in the gabbro and of fluoride in Barre and Westerly either remain the same or increase during the experiments, indicating a mineral source for these ions.

OTHER INVESTIGATIONS

Many countries are presently investigating the possibility of disposing high-level nuclear waste in crystalline rock types such as granite. Because of this, several studies have been conducted to determine the effects of heated groundwater on rock properties. Such studies are also important for understanding geothermal systems, including hot dry rock systems. Present investigations on these topics are of three types: (1) chemical analyses of natural groundwaters collected at depth (*e.g.*, Frape *et al.*, 1984; Nordstrom *et al.*, 1984); (2) fluid-rock interaction experiments at elevated temperatures (*e.g.*, Bourg *et al.*, 1985; Grigsby *et al.*, 1983; Savage, 1986; Charles and Bayhurst, 1983); and (3) determination of the paths fluids take through rock (*e.g.*, Katsube and Kamineni, 1983). These investigations have bearing on the interpretation of the results of our permeability experiments.

Nordstrom *et al.* (1984) analyzed groundwaters collected at depths to 880 meters from the Stripa granite in Sweden. They found that calcium, sodium, bromide, and iodide concentrations in the fluids are directly correlated with chloride concentrations, which suggests a similar source for all these ions. The saline content of the waters does not show a simple increase with depth, and groundwaters collected from closely spaced fracture systems often have very different compositions. Nordstrom *et al.* (1984) concluded that the deeper groundwaters are a mixture of fresh water with varying amounts of a saline component that was derived locally from breached fluid inclusions.

Frape et al. (1984) analyzed groundwaters collected from mining districts of the Canadian Shield. They proposed that the groundwater compositions are a function of two major processes: (1) rock-water interaction, and (2) mixing of waters from different sources. The chemistry of the shallower groundwaters is correlated with the rock type, such that the waters associated with mafic rocks show the relations Ca>Mg>Na and HCO_3>Cl = SO_4, whereas the groundwaters collected from granitic rocks have the composition Na>Ca>Mg>K and HCO_3>SO_4>Cl. These relationships suggest the influence of mineral dissolution on groundwater composition. Frape et al. (1984) also measured a marked increase in groundwater salinity with increasing depth; these deep saline waters apparently are affected by complex rock-water interactions involving mineral precipitation as well as dissolution. Based on isotopic analyses, they determined that many of the groundwaters represent mixtures of fresh surface waters and the deeper saline brines.

Grigsby et al. (1983) measured fluid chemistry changes during a test run of a hot dry rock facility in the Jemez Mountains of northern New Mexico. Granitic rock at depth between two wells was hydraulically fractured. Water was injected into one well, whereupon it flowed through the fractured granitic rock into the second well. The water was then extracted from the second well and reinjected into the first well. The early-recovered fluids contained high concentrations of dissolved materials, which they interpreted to represent displaced indigenous pore fluids. These concentrations dropped rapidly as a result of dilution by the injected water. The concentrations of dissolved species in the fluids sampled at later times during the test were in part a function of the amount of contact time between the water and the reservoir rock.

Savage (1986) measured fluid chemistry changes resulting from the interaction of water with ground granite during experiments conducted at 100°C for a period of 203 days. He found that silica, potassium, and calcium concentrations reached steady-state values during the experiments, which he attributed to buffering by the solubility of quartz, muscovite and/or K-feldspar, and calcite, respectively. The concentrations of species such as sodium and aluminum did not reach steady-state values; the amounts of these ions in solution were apparently controlled by the kinetics of reactions involving albite and plagioclase.

Bourg et al. (1985) also investigated granite-water interaction, using a technique that combined elements of our permeability experiments and the hydrothermal experiments of Savage (1986). Distilled water heated to 80°C was first passed through a column filled with granite powder and then through a fractured granite cylinder that was held in a temperature gradient of 80°-50°C. After the experiment, SEM examination of the fracture surface showed evidence of dissolution and also of the precipitation of silicate coatings similar to those illustrated in Morrow et al. (1981). They also conducted leaching experiments at 50° and 100°C reacting granite powders of various size fractions with water. A third set of experiments was held initially at 100°C for several days and then cooled to 50°C and run at that temperature for several additional days. Bourg et al. (1985) suggested that feldspar rather than quartz was the source of silica coming into solution during the granite leaching experiments. They did consider, however, that some form of silica, perhaps chalcedony, may have precipitated during the experiments run under declining temperatures. Minerals such as kaolinite, montmorillonite, or illite may have precipitated along with the silica phase.

Charles and Bayhurst (1983) constructed a recirculating hydrothermal system, in which small polished samples of biotite granodiorite were placed at intervals in a pressure vessel with an imposed temperature gradient (room temperature to 310°C). Distilled water was pumped from low to high temperatures through the pressure vessel at the relatively rapid rate of 3 cm^3/min for a period of 60 days. The water was allowed to cool as it was pumped back to the low-temperature side of the pressure vessel. At the end of the experiment, the granodiorite samples that had been placed at temperatures below 120° showed a slight weight gain due to mineral precipitation. With increasing temperature between 120° and 310°C, however, the samples showed progressively greater amounts of net weight loss, which was due principally to the dissolution of quartz. The fluids discharged from the high-temperature side of the pressure vessel nevertheless had dissolved silica concentrations that were well below quartz saturation at 310°C. Some microcline was also dissolved at the higher temperatures. Electron microprobe analyses of plagioclase crystals on the sample surfaces showed a slight decrease in their calcium contents, which indicates preferential leaching of the anorthite component of the plagioclase. Biotite was resistant to leaching, and it formed ridges on the corroded, high-temperature samples. The types of secondary phases deposited on the granodiorite samples during the experiment varied with temperature. Below 120°C, the principal mineral precipitate had a composition similar to the Ca-montmorillonite beidellite. At 160°C, the precipitate was similar in composition to the zeolites heulandite and stilbite, and at temperatures above 200°C the zeolite thomsonite may have crystallized. Charles and Bayhurst (1983) explained the observed sequence of secondary minerals as a function of both increasing temperature and decreasing chemical potential of silica.

Katsube and Kamineni (1983) studied the effects of natural alteration on the pore structure of a granitic pluton from the Canadian Shield. The rocks show partial replacement of hornblende, biotite, and plagioclase by the secondary minerals epidote, sericite, chlorite, carbonate, and minor hematite, sphene, and quartz. The permeability of unaltered samples of the granodiorite was in the range 6-20 microdarcies (μda). With increasing degrees of alteration in the granite, they found a corresponding increase in the tortuosity and decreases in the connecting porosity, the permeability, and to some extent the effective porosity. Katsube and Kamineni (1983) explained these changes as due to alteration under declining temperature conditions, during late magmatic and hydrothermal stages. During the earlier, higher temperature stage, selective dissolution of minerals caused localized enlargement of the pore channels (pocket pores). As temperatures gradually declined, the fluids became supersaturated and minerals were deposited all along the channels, thereby reducing their apertures. The rearrangement of minerals along the pore networks causes the observed changes in permeability and tortuosity. Alteration reactions such as those observed in the granite are generally accompanied by an increase in volume, which leads to the observed reductions in porosity.

COMPARISON OF RESULTS

All the experimental studies cited above were conducted on granite-water systems. The experiments of Savage (1986) and Bourg *et al.* (1985) were run at lower temperatures than those of this study. Nevertheless, Savage (1986) comes to conclusions about the sources of species in solution similar to those proposed in this study for granitic rocks. Bourg et al. (1985) suggest, instead, that feldspar rather than quartz is the principal source of dissolved silica. The experiments on rock types other than granite or granodiorite in this study indicate, however, that this conclusion of Bourg et al. (1985) is incorrect. Both the gabbro and anorthosite, which contain plagioclase without either K-feldspar or quartz, showed considerably lower dissolved silica concentrations than the granodiorite and quartzite samples (Fig. 13). Therefore, plagioclase can contribute only a small part of the dissolved silica content of heated granitic waters. The quartzite and the three granodiorite samples had similar dissolved silica contents (Fig. 13), which suggests a similar source. The quartzite may once have contained traces of K-feldspar (Table 1), but that mineral has since altered to muscovite. Therefore, quartz is the principal source of dissolved silica in the quartzite, and it may be the major source in Barre and Westerly as well. At the lower temperatures of the experiments of Bourg et al. (1985), the solubilities of both quartz and the feldspars will decrease, but quartz should still be more highly soluble than either of the feldspars. The experimental results of Charles and Bayhurst (1983) support the conclusions of Morrow et al. (1985), Savage (1986), and this study for the sources of dissolved silica. Quartz was by far the most highly reactive mineral in their granodiorite samples, being completely removed from the highest temperature samples.

According to Frape et al. (1984), the compositions of near-surface natural groundwaters, particularly the cations, should be a function of the host rock mineralogy. Although diluted with deionized water, the room-temperature fluid samples from our experiments (Table 6) should reflect the relative proportions of dissolved species in groundwaters of those rock types. The following relative mole percentage abundances were obtained for the room-temperature fluid samples of the five rock types studied:

Anorthosite---	Na>K>Ca>Mg	$HCO_3>Cl>SO_4>F$
Gabbro---	Na>K>Ca>Mg	$HCO_3>Cl>SO_4\geq F$
Westerly---	Na>Ca>K>>Mg	$HCO_3>Cl>SO_4>F$
Barre---	Na>Ca>K>>Mg	$HCO_3>SO_4>Cl>>F$
Quartzite---	Na>K>Ca>Mg	$HCO_3>SO_4>Cl>F$

Where possible, the ranking for each rock type was made for the most concentrated fluid sample collected during the room-temperature run. Except for sulfate in Westerly and magnesium in both Barre and Westerly, the granodiorite ionic abundances show a good correspondence to the granitic groundwater compositions of Frape et al. (1984), that were listed earlier. The relatively high sodium and potassium contents compared to calcium and magnesium in the anorthosite and gabbro fluids, however, do not correspond to the groundwater compositions of the mafic Canadian Shield rocks.

The relative molar abundances of the final heated fluid samples of the six experiments were also obtained:

Anorthosite---	Na>K>Ca>Mg	$HCO_3>Cl>F>SO_4$
Gabbro---	Na>>K≥Mg = Ca	$HCO_3>>Cl>SO_4>F$
Westerly---	Na>Ca>>K>Mg	$HCO_3>Cl>F>SO_4$
Barre-1---	Na>Ca>K>>Mg	$Cl\geq HCO_3>F>SO_4$
Barre-2---	Na>Ca>K>>Mg	$HCO_3>Cl>F>SO_4$
Quartzite---	Ca>Na>K>Mg	$HCO_3>SO_4>Cl>F$

This set of relative compositions is only slightly different from the room-temperature set, although the absolute concentrations of each ion can be quite different after heating. The principal change is the decreased importance of sulfate among the anions of some of the samples, which is probably due to the lack of a mineral source of sulfate in those rocks. In quartzite, calcium replaces sodium as the most abundant cation, probably as a result of calcite dissolution.

The results of Katsube and Kamineni (1983) illustrate the types of changes in pore and crack geometry that may have occurred in our heated rock cylinders. The fluid chemistry results of Grigsby et al. (1983) from a natural system are very similar to our experimental results. They found that the early-collected fluids from their hot dry rock test contained a large component of granitic pore waters, whereas the later-collected fluids reflect the dissolution of minerals in the reservoir rock. The work of Nordstrom et al. (1984) shows that fluid inclusions may also contribute to natural pore fluid compositions, in agreement with Moore et al. (1983).

CONCLUSIONS

The conclusions of Moore et al. (1983) and Morrow et al. (1985) on permeability and fluid chemistry of the crystalline rock permeability experiments have been summarized on pages 21, 25, and 33. Additional conclusions resulting from this study are summarized below:

(1) The initial permeabilities of the crystalline rocks studied are functions of rock type and textural properties, most notably the degree of development and filling of fractures.

(2) Previously suggested correlations between mineral and fluid chemistry relative to magnesium and sodium-to-calcium ratios (Moore et al., 1983) do not hold when all five rock types are considered.

(3) Quartz is the major source of dissolved silica; calcite, where present, is the major source of calcium and bicarbonate. Relatively high magnesium concentrations in some calcite-bearing samples are attributed to solid solution of magnesium in the calcite. Feldspars and muscovite may control the amounts of sodium and potassium in solution.

(4) The variations with time of silica and calcium concentrations in the discharged fluids suggest that they may have been increasingly involved in precipitation reactions as well as dissolution reactions, as permeability decreased.

REFERENCES

Bourg, A. C. M., Oustriere, P., and Sureau, J. F., 1985. Experimental investigation of clogging of fissures and pores in granite. Mineral Mag. 49, 223-231.

Charles, R. W., and Bayhurst, G. K., 1983. Rock-fluid interactions in a temperature gradient: Biotite granodiorite + H_2O. Jour. Volcanology and Geothermal Res. 15, 137-166.

Frape, S. K., Fritz, P., and McNutt, R. H., 1984. Water-rock interaction and chemistry of groundwaters from the Canadian Shield. Geochim. Cosmochim. Acta 48, 1617-1627.

Grigsby, C. O., Tester, J. W., Trujillo, P. E., Counce, D. A., Abbott, J., Holley, C. E., and Blatz, L. A., 1983. Rock-water interactions in hot dry rock geothermal systems: Field investigations of in situ geochemical behavior. Jour. Volcanology and Geothermal Res. 15, 101-136.

Grout, F. F., and Schwartz, G. M., 1939. The geology of the anorthosites of the Minnesota coast of Lake Superior. Minnesota Geol. Surv. Bull. 28, 119 pp.

Katsube, T. J., and Kamineni, D. C., 1983. Effect of alteration on pore structure of crystalline rocks: core samples from Atikokan, Ontario. Canad. Mineralogist 21, 637-646.

Moore, D., Morrow, C., and Byerlee, J., 1983. Chemical reactions accompanying fluid flow through granite held in a temperature gradient. Geochim. Cosmochim. Acta 47, 445-453.

Moore, D. E., Morrow, C. A., and Byerlee, J. D., 1986. High-temperature permeability and ground water chemistry of some Nevada Test Site tuffs. Jour. Geophys. Res. 91, 2163-2171.

Morrow, C., Lockner, D., Moore, D., and Byerlee, J., 1981. Permeability of granite in a temperature gradient. Jour. Geophys. Res. 86, 3002-3008.

Morrow, C., Moore, D., and Byerlee, J., 1985. Permeability changes in crystalline rocks due to temperature: Effects of mineral assemblage. Proc. Mater. Res. Soc. Symp. 8, 467-474.

Nordstrom, D. K., 1984. Geochemical investigations on the Stripa groundwaters. Presented at: GSF, Munich-Neuhenberg, Stripa Hydrogeochemical Advisory Group Meeting, June 6, 1984.

Savage, D., 1986. Granite-water interactions at 100°C, 50 MPa: An experimental study. Chem. Geol. 54, 81-95.

Taylor, R. B., 1964. Geology of the Duluth Gabbro Complex near Duluth, Minnesota. Minnesota Geol. Surv. Bull. 44, 63 pp.

Vaughan, P. J., Moore, D. E., Morrow, C. A., and Byerlee, J. D., 1986. Role of cracks in progressive permeability reduction during flow of heated aqueous fluids through granite. Jour. Geophys. Res. 91, 7517-7530.